Early evidence of the genus *Homo* in East Asia

R.X. Zhu [a,*], R. Potts [b,*], Y.X. Pan [a], H.T. Yao [a], L.Q. Lü [a], X. Zhao [a], X. Gao [c], L.W. Chen [d], F. Gao [e], C.L. Deng [a]

[a] *Paleomagnetism and Geochronology Laboratory (SKL-LE), Institute of Geology and Geophysics, Chinese Academy of Sciences, Beijing 100029, China*
[b] *Human Origins Program, National Museum of Natural History, Smithsonian Institution, Washington, DC 20013-7012, USA*
[c] *Institute of Vertebrate Paleontology and Paleoanthropology, Chinese Academy of Sciences, Beijing 100044, China*
[d] *The Geological Museum of China, Beijing 100034, China*
[e] *Yunnan Cultural Relics and Archeology Institute, Kunming 650118, China*

ARTICLE INFO

ABSTRACT

The timing and route of the earliest dispersal from Africa to Eastern Asia are contentious topics in the study of early human evolution because Asian hominin fossil sites with precise age constraints are very limited. Here we report new high-resolution magnetostratigraphic results that place stringent age controls on excavated hominin incisors and stone tools from the Yuanmou Basin, southwest China. The hominin-bearing layer resides in a reverse polarity magnetozone just above the upper boundary of the Olduvai subchron, yielding an estimated age of 1.7 Ma. The finding represents the age of the earliest documented presence of *Homo*, with affinities to *Homo erectus*, in mainland East Asia. This age estimate is roughly the same as for *H. erectus* in island Southeast Asia and immediately prior to the oldest archaeological evidence in northeast Asia. Mammalian fauna and pollen obtained directly from the hominin site indicate that the Yuanmou hominins lived in a varied habitat of open vegetation with patches of bushland and forest on an alluvial fan close to a lake or swamp. The age and location are consistent with a rapid southern migration route of initial hominin populations into Eastern Asia.

© 2008 Elsevier Ltd. All rights reserved.

Introduction

Human evolution involved a substantial geographic expansion of early hominin populations into new landscapes and climate regimes beyond Africa. The oldest known dispersal of the genus *Homo* into Eurasia is a benchmark of this expansion and, presumably, of the human capacity to adapt to novel environments. The timing and likely geographic route of the earliest dispersal from Africa to Eastern Asia, in particular, are contentious topics because Asian hominin fossil sites with precise age constraints are very limited (Swisher et al., 1994; Gabunia et al., 2000a; Larick et al., 2001; Vekua et al., 2002; Dennell, 2003; Antón and Swisher, 2004; Dennell and Roebroeks, 2005). Here we address these questions by presenting paleomagnetic dating of the hominins, vertebrate fauna, and paleoenvironments in the Yuanmou Basin, southwest China.

Geological and archaeological settings

Lithostratigraphy and mammalian fossils

The Yuanmou Basin is located near the southeastern margin of the Tibetan Plateau with an elevation of 1,000 to 1,400 m, 110 km northwest of Kunming City, Yunnan Province (Fig. 1). The late Cenozoic Yuanmou Formation consists of four lithologic members, from oldest to youngest: lacustrine and fluviolacustrine silty clay, silts, and fine-grained sands (M1); fluvial and fluviolacustrine peaty clays, silts, silty clays, and fine-grained sands (M2); fluvial silty clays interbedded with silts and fine-grained sands (M3); and fluvial and alluvial silty clays interbedded with sandy conglomerates (M4); (Pu and Qian, 1977; Qian and Zhou, 1991). M4 is rich in mammalian fossils (see Table 1) known as the Yuanmou Fauna (Bien, 1940) and includes two hominin incisors found in 1965 by Qian Fang (Hu, 1973; Qian et al., 1984). The mammalian assemblage is similar taxonomically to the early Pleistocene Nihewan Fauna in north China and the Villafranchian Fauna in Europe (Bien, 1940; Pei, 1961; Hu, 1973; Qiu, 2000; Deng et al., 2008).

Mammalian fossils were excavated in 1973 from M4 at the Niujianbao (NJB; red star in Fig. 1) section (25°40.690′N, 101°54.732′E). The level of the hominin incisors is near the bottom of the NJB section. Fossils of biochronologically useful species recovered in the hominin site include Pliocene survivors, such as *Nestoritherium* (*Hesperotherium*) sp., *Cervocerus ultimus*, *Procapreolus stenosis*, *Eostyloceros longchuanensis*, *Paracervulus attenuatus*, and *Stegodon elephantoides*, and taxa typical of the early Pleistocene of China, such as *Hyaena licenti*, *Equus yunnanensis*, *Muntiacus lacustris*, *Megantereon nihowanensis*, and *Rusa yunnanensis* (Table 1).

* Corresponding authors.
E-mail addresses: rxzhu@mail.iggcas.ac.cn (R.X. Zhu), pottsr@si.edu (R. Potts).
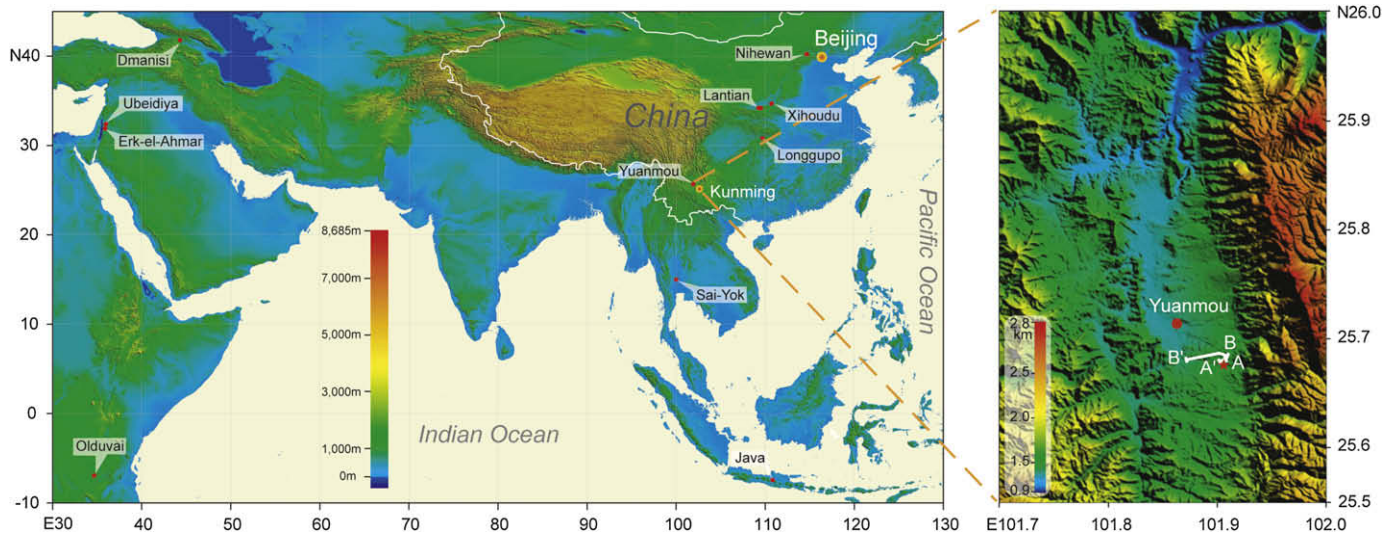
Fig. 1. Geographic map showing the location of the Yuanmou Basin. Other hominin and Paleolithic sites in Eurasia and East Africa are also shown. The hominin site (red star) and two sampling sections in the Yuanmou Basin, named Niujianbao (NJB, A–A') and Dapoqing (DPQ, B–B'), are marked.

The dentition

The left and right upper central incisors, labelled V1519 (Fig. 2), have previously been described and attributed to *Homo (Sinanthropus) erectus yuanmouensis* (Hu, 1973; Wu and Poirier, 1995). These incisors lack a cervical cingulum, large expansion of the cervical half of the lingual surface, and the overall splaying or rounded arch typical of the I^1 crowns of extant great apes (Pilbrow, 2006). Their dimensions also fall outside the 95% confidence intervals determined from the large sample of I^1 crowns known for *Lufengpithecus*, a late Miocene ape from southwest China, including older sediments in the Yuanmou Basin (Wood and Xu, 1991; Liu et al., 2000).

In their dimensions, overall morphology, details of enamel wrinkling, expression of the basal tubercle, and shovelling of the lateral margins on the lingual surface, the Yuanmou incisors are nearly identical to upper central incisors of *H. erectus* from Zhoukoudian, China (e.g., specimen PA 66). The overall and detailed morphology also strongly resemble early African *H. erectus* sensu lato (e.g., KNM-WT 15000, which exhibits a lingual basal swelling, central pillar [on left I^1] and strong enamel wrinkling similar to that observed on the Yuanmou teeth). Well-preserved Plio-Pleistocene I^1 specimens are very rare, however. It is thus relevant to note similarities between the Yuanmou incisors and a left I^1 from Koobi Fora (KNM-ER 1590B) associated with a cranial vault attributed to *H. habilis* (Wood, 1991; Table 2).

An attribution of the Yuanmou incisors to early *Homo* sp. thus seems appropriate to us based on these observations and findings elsewhere, such as the species-level taxonomic uncertainty of the Dmanisi material (Lordkipanidze et al., 2007), the fragmentary nature of possible *H. erectus* material from the lower Sangiran Formation, Java (Antón and Swisher, 2004), and the primitive wrist morphology recorded much later in *H. floresiensis* (Flores, Indonesia) with similarities to African Pliocene hominins (Tocheri et al., 2007). We recognize that a provisional attribution to *H. erectus* sensu lato is also defensible until more complete discoveries of similar age at Yuanmou or nearby might improve the taxonomic interpretation.

Stone artifacts

Excavations at the same site and in the same strata in 1973 by the Institute of Vertebrate Paleontology and Paleoanthropology

(Academia Sinica), the Yunnan Province Museum, and the Yuanmou Man Exhibition Hall yielded four in situ stone artifacts dispersed ∼20 m horizontally (Fig. 2); their vertical dispersion of ∼1.5 m encompasses the incisors-bearing layer (Wen, 1978; Yuan et al., 1984). These four stone artifacts from the 1973 excavation include a unifacial scraper, a small bifacial core, and two flakes. The artifacts, which were made on small quartz cobbles, were outsized clasts excavated in silty clay sediment, have overlapping flake scars, and show platform edge and flake scar morphologies that are indicative of precise stone-on-stone percussion (Wen, 1978; Yuan et al., 1984). Both the scraper and bifacial core are <60 mm in maximum dimension, and the most distinct flake scars on each are <30 mm in length. The scraper has a minimum of eight overlapping flake scars. The two flakes show thin terminations and thicker platform ends, yet the bulbs of percussion are poorly developed. The dorsal surface of one of the flakes exhibits several facets that may reflect flake scars indicative of more than one generation of percussion flaking. The small size of the artifacts, the relatively few distinct yet overlapping flake scars, and the characteristics of the flakes are all quite similar to African Oldowan artifacts made of quartz or quartzite. No artifacts have been reported from other portions of the NJB section. Despite intensive paleoanthropological and geological investigation, the Yuanmou site and laterally equivalent strata lack any evidence of dense artifact concentrations even though this area of the basin is well-dissected by erosion. The apparent low density of artifacts at Yuanmou could reflect a low degree of dependence on stone technology, a very low population density, or a relatively brief stop by hominins as they passed through the area.

Previous paleomagnetic dating of the Yuanmou incisors and artifacts

Previous paleomagnetic studies of the Yuanmou sequence were reviewed in detail by Zhu et al. (2003). Among those studies, two representative paleomagnetic investigations of the sequence have yielded ambiguous results and implied age estimates for the hominin remains that differed by nearly 1 million years (Li et al., 1976; Hyodo et al., 2002). Li et al.'s (1976) results showed that the Yuanmou incisors occurred within a tiny reverse polarity magnetozone bracketed by normal polarity magnetozones. The three magnetozones were interpreted to be the Gilsa normal event,

Table 1
Mammalian and animal fossils and sporopollen from the Yuanmou Man site (with asterisk) and Member 4 of the Yuanmou sequence[a]

Mammalian fossils	Age/bed number	References
Nestoritherium (*Hesperotherium*) sp.*	Tertiary/#25	Yuan et al. (1984)
*Cervocerus ultimus**	Tertiary/#25–27	Yuan et al. (1984); Lin et al. (1978)
*Procapreolus stenosis**	Tertiary/#25–27	Yuan et al. (1984); Qian and Zhou (1991)
Eostyloceros longchuanensis	Tertiary/#26	Pu and Qian (1977); Lin et al. (1978)
Paracervulus attenuatus	Tertiary/#25	Pu and Qian (1977); Lin et al. (1978)
Stegodon elephantoides	Tertiary/#26	Pu and Qian (1977); Lin et al. (1978)
Muntiacus lacustris	early Pleistocene/#25	Pu and Qian (1977); Lin et al. (1978)
*Equus yunnanensis**	early Pleistocene/#24–27	Yuan et al. (1984); Hu (1973)
Hyaena licenti	early Pleistocene/#25	Pu and Qian (1977); Lin et al. (1978)
Megantereon nihowanensis	early Pleistocene/#24	Pu and Qian (1977); Lin et al. (1978); Qian and Zhou (1991)
*Rusa yunnanensis**	early Pleistocene/#25	Yuan et al. (1984)
Cervus (*Rusa*) *stehlini**	#25	Yuan et al. (1984)
Metacervulus capreolinulus	#26	Pu and Qian (1977); Lin et al. (1978)
Axis cf. *rugosus*	#27	Pu and Qian (1977); Lin et al. (1978)
Axis sp.*	#25	Yuan et al. (1984)
Muntiacus nanus	#25	Pu and Qian (1977)
Bos sp.*	#24–27	Yuan et al. (1984)
Gazella sp.*	#25	Yuan et al. (1984)
Bovidae*	#25	Hu (1973)
Cervus sp.*	#24–26	Hu (1973); Lin et al. (1978)
Sus sp.*	#25–27	Yuan et al. (1984)
Stegodon sp.*	#24,25	Hu (1973); Yuan et al. (1984)
Rhinoceros sp.*	#25,27	Lin et al. (1978); Qian and Zhou (1991)
*Hystrix subcristata**	#25	Yuan et al. (1984)
Rhizomys sp.*	#25	Yuan et al. (1984)
Microtus sp.*	#25	Hu (1973); Lin et al. (1978)
Rodentia indet.*	#25	Hu (1973)
Bos (*Bibos*) sp.		Lin et al. (1978)
Bubalus sp.		Pu and Qian (1977)
Rusa sp.	#26	Pu and Qian (1977); Lin et al. (1978)
Rhinoceros sinensis	#25,27	Pu and Qian (1977); Lin et al. (1978)
Panthera tigris	#24	Qian and Zhou (1991)
Viverricula malaccensis fossilis	#26	Pu and Qian (1977); Lin et al. (1978)
Ochotonoides complicidens	#25	Pu and Qian (1977); Lin et al. (1978)
Arvicola sp.	#25	Pu and Qian (1977); Lin et al. (1978)

Molluscan fossils	Bed number	
Gastropoda*	#25	Yuan et al. (1984)
Radix sp.*	#25–27	Pu and Qian (1977); Qian and Zhou (1991)
Viviparus sp.*	#25–27	Pu and Qian (1977); Qian and Zhou (1991)
Cathaica sp.*	#25	Pu and Qian (1977)
Gyraulus sp.*	#25	Pu and Qian (1977)
Corbicula sp.*	#25,26	Pu and Qian (1977)

Other fauna		
Cyriuus caspio	#25	Pu and Qian (1977)
Testudo sp.	#25	Pu and Qian (1977)
Amyda sp.	#25	Qian and Zhou (1991)
Ilyocypris aspera Gall	#24	Qian and Zhou (1991)
I.dunschanensis Mandelstam	#24	Qian and Zhou (1991)
I. gibba Ramdohr	#24	Qian and Zhou (1991)
Neocypridopsis simpex Huang	#24	Qian and Zhou (1991)
Potomocypris smaragdina Vavra	#25	Qian and Zhou (1991)
Ilyocypris bradyi Sars	#26,28	Qian and Zhou (1991)
Candona sp.	#24,27	Qian and Zhou (1991)
Candoniella albicans Brady	#24,27,28	Qian and Zhou (1991)

Table 1 (*continued*)

Mammalian fossils	Age/bed number	References
Candoniella mirabilis Schneider	#27	Qian and Zhou (1991)
Metacypris lijiangenesis Huang	#27	Qian and Zhou (1991)
Pollen: tree		
Pinus	#24–28	Pu and Qian (1977)
Podocarpus	#24,25	Qian and Zhou (1991)
Ulmus	#24,25	Qian and Zhou (1991)
Quercus	#24–28	Qian and Zhou (1991)
Moraceae	#24,26–28	Qian and Zhou (1991)
Alnus	#25–28	Qian and Zhou (1991)
Juglans	#25,26	Qian and Zhou (1991)
Castanopsis	#25	Qian and Zhou (1991)
Acer	#25	Qian and Zhou (1991)
Betula	#25–28	Qian and Zhou (1991)
Myrtaceae	#25	Qian and Zhou (1991)
Osmanthus	#25	Qian and Zhou (1991)
Apocynaceae	#25	Qian and Zhou (1991)
Larix	#25	Qian and Zhou (1991)
Cedrus	#25,26	Qian and Zhou (1991)
Cupressaceae	#25	Qian and Zhou (1991)
Magnoliaceae	#25	Qian and Zhou (1991)
Leguminosae	#25	Qian and Zhou (1991)
Carpinus	#25,27	Qian and Zhou (1991)
Pterocarya	#25	Qian and Zhou (1991)
Proteaceae	#25	Pu and Qian (1977)
Carya	#26	Qian and Zhou (1991)
Picea	#26	Qian and Zhou (1991)
Abies	#26	Qian and Zhou (1991)
Corylus	#26	Qian and Zhou (1991)
Rhus	#26	Qian and Zhou (1991)
Meliaceae	#26	Qian and Zhou (1991)
Myrica	#27	Qian and Zhou (1991)
Pollen: bush and grass		
Liliaceae	#24	Qian and Zhou (1991)
Chenopodiaceae	#24–28	Pu and Qian (1977)
Artemisia	#24,26–28	Pu and Qian (1977)
Gramineae	#25,26,28	Pu and Qian (1977)
Ranunculaceae	#25	Qian and Zhou (1991)
Capparidaceae	#25	Qian and Zhou (1991)
Compositae	#25	Qian and Zhou (1991)
Rosaceae	#27	Qian and Zhou (1991)
Spore: fern		
Polypodiaceae	#24,25	Qian and Zhou (1991)
Pteris	#24,25	Qian and Zhou (1991)
Botrychium	#24	Qian and Zhou (1991)
Angiopteris	#24	Qian and Zhou (1991)
Polypodium	#24	Qian and Zhou (1991)

[a] Member 4 consists of Bed #24 through #28 (from bottom to top). Bed no. (#) is based on the lithologic units described by Qian and Zhou (1991). Two hominin incisors were excavated from the middle part of Bed #25 from Member 4 at NJB section (25°40.690′N, 101°54.732′E).

which has an estimated age of 1.7 Ma (Worm, 1997), and those portions of the Matuyama reverse chron that border it. By contrast, a more recently reconstructed magnetostratigraphy of the Yuanmou sequence placed the incisors above the Matuyama-Brunhes boundary (Hyodo et al., 2002), which has most recently been dated at 0.78–0.79 Ma (Singer et al., 2002). In the first study by Li et al. (1976), samples were not analyzed by stepwise thermal demagnetization, which is now standard practice in evaluating sediments that contain hematite as a principal remanence carrier. In the more recent work by Hyodo et al. (2002), paleomagnetic analysis of the upper 88 m of M4 involved only six sampling levels, and the sampling route was about 600 m north of the hominin site (see Fig. 1 of Hyodo et al., 2002). For these reasons, the earlier studies cannot adequately resolve the age of the Yuanmou evidence of *Homo*; a more thorough magnetostratigraphic study directly associated with the hominin fossil site is required. In this study, we
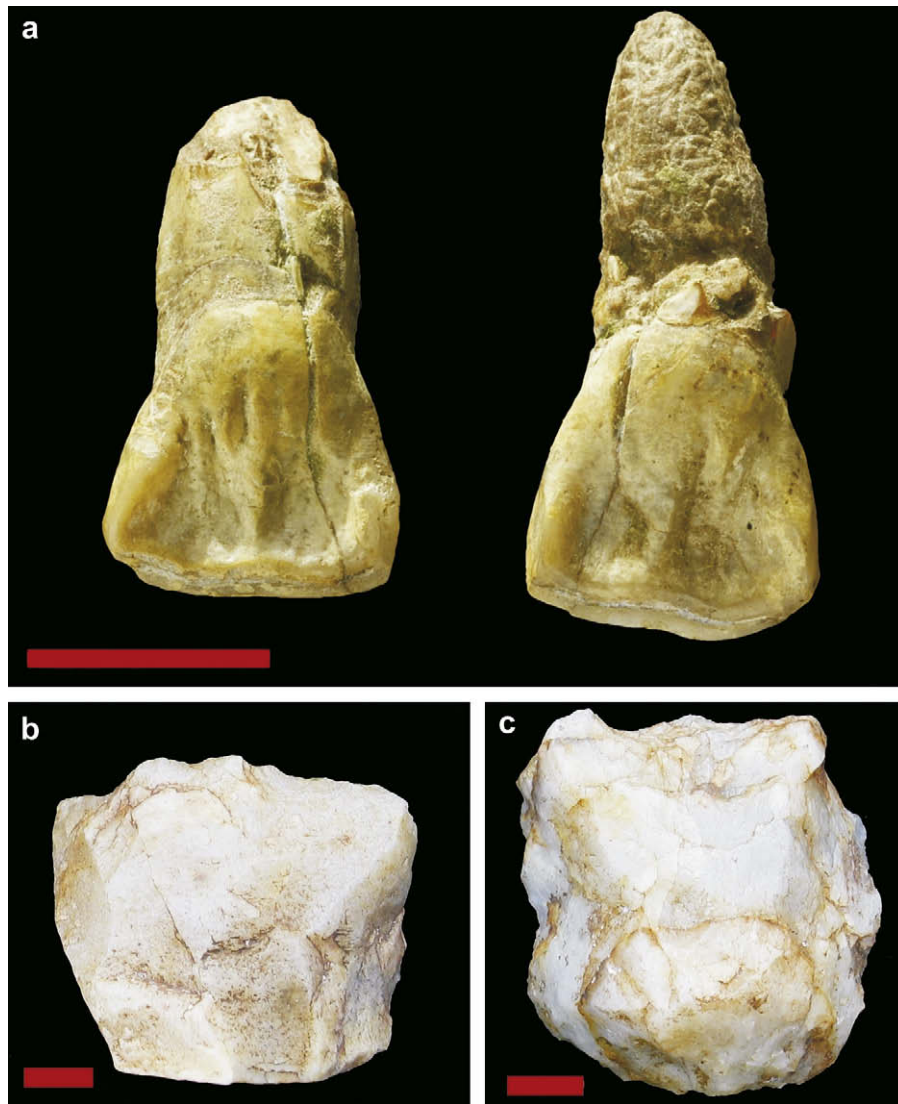
Fig. 2. Hominin left and right upper central incisors (a) from the Yuanmou Man site. Mesiodistal and labiolingual crown diameters: 11.4 and 8.1 mm for the left I[1], 11.5 and 8.6 mm for the right I[1]. Their size, overall morphology, and detailed enamel features are an excellent match for upper central incisors of middle Pleistocene *H. erectus* from Zhoukoudian, early Pleistocene African *H. erectus* sensu lato (KNM-WT 15000), and have strong similarities to late Pliocene African *H. habilis* (KNM-ER 1590B). Quartz stone artifacts recovered by excavation include a unifacial scraper (b) and small bifacial core (c), both with multiple, overlapping flake scars, and two flakes.

present a high-resolution magnetostratigraphic study of the NJB sequence based on detailed rock magnetic investigation (Fig. 3) and progressive thermal demagnetization (Fig. 4). Our new magneto-stratigraphic findings place stringent age controls on excavated hominin incisors and stone tools from the Yuanmou Basin (Fig. 5).

Table 2
Dimensions of the Yuanmou left and right upper central incisors, compared to specimens of East African *Homo* that exhibit strong similarities in their detailed morphology (see text)[a]

	Yuanmou (left)	Yuanmou (right)	KNM-WT 15000 (left)	KNM-WT 15000 (right)	KNM-ER 1590B (left)
Mesiodistal crown diameter	11.4	11.5	12.0	11.5	12.3
Labiolingual crown diameter	8.1	8.6	9.3	9.4	7.7

[a] KNM-WT 15000 is most commonly ascribed to *Homo erectus* sensu lato (Walker and Leakey, 1993), while KNM-ER 1590B is associated with a cranial vault that has been ascribed to *Homo habilis* (Wood, 1991). Repeated measurements of the specimens agreed with those reported previously (Wood, 1991; Walker and Leakey, 1993; Wu and Poirier, 1995). Measurements in mm.

Paleomagnetic sampling

To determine the age of the hominin incisors and artifacts, we first paleomagnetically examined the entire 79.2-m-thick NJB section (see A–A' in Fig. 1) about 160 m north of the hominin incisors and artifact site. One hundred ninety-eight oriented block samples were collected from the NJB section at about 0.4 m intervals. The incisors-bearing layer corresponds to the 59–60.5 m depth interval in this section (Fig. 5).

Because previous excavation removed the 4-m-high hill in which the hominin incisors were found, we then conducted parallel samplings on nearby hills at the same elevation to test for concordant results that could be used as a proxy for the magnetostratigraphic sequence of the missing hill. A monument marks the hill base where the hominin incisors were found (Fig. 6). In order to examine the magnetic polarity of the hominin-bearing profile, in 2003 we dug a 21-m-deep well on a hill that is about 30 m east of the monument (see Fig. 6a). The well covers an interval of 3 m above the zero level (referred to the monument base level here) and 18 m beneath it. Ninety-eight block oriented samples were collected at 0.2 m intervals. In 2005, 23 block oriented
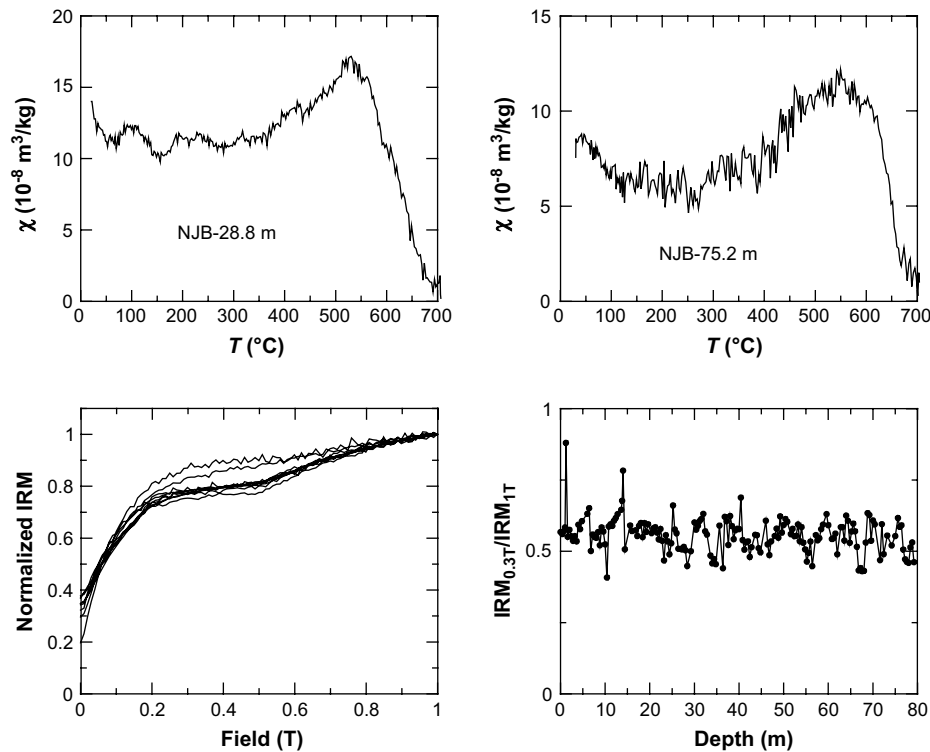
Fig. 3. Rock magnetic measurements of the NJB section: (upper graphs) high-temperature magnetic susceptibility (χ–T) of selected samples, (lower left) IRM acquisition curves for selected samples, and (lower right) the $IRM_{0.3T}/IRM_{1T}$ ratio of the whole NJB section.

samples at 0.2–0.4 m intervals were taken from another outcrop section (see Fig. 6b), which has an equivalent height as the removed hill and is about 20 m west of the monument. The top of the section is about 3 m higher than the zero level. A total of 319 oriented block samples (221 from the outcrop and 98 from the well) were collected. Cubic specimens of 20 mm $\times$ 20 mm $\times$ 20 mm were obtained from those block samples in the laboratory.

Methodology

Rock magnetic measurements

Rock magnetic investigations included high-temperature magnetic susceptibility (χ–T) and isothermal remanence. χ–T curves were measured on selected samples using a KLY-3 Kappabridge with a CS-3 high-temperature furnace (Agico Ltd., Brno) in an argon atmosphere. The sample holder and thermocouple contributions to magnetic susceptibility were subtracted. Isothermal remanent magnetizations (IRMs) for each selected sample were imparted from 0 to 1.0 T using a MicroMag 2900 Alternating Gradient Magnetometer (Princeton Measurements Corp., USA). IRMs of all the NJB outcrop samples were produced using a Model 670 IRM Impulse Remanent Magnetizer (2G Enterprises, USA) in steady constant fields of 0.3 T and 1.0 T, and then measured using a three-axis cryogenic magnetometer (2G Enterprises, USA).

Paleomagnetic measurements

In order to establish the magnetic polarity stratigraphy, the natural remanent magnetization (NRM) of one specimen per sampling level was subjected to stepwise demagnetization. All of the 319 samples were subjected to progressive thermal demagnetization (12–21 steps) up to a maximum temperature of 685 °C with

25–50 °C intervals below 585 °C and 10 °C above 585 °C using a Magnetic Measurements thermal demagnetizer with a residual magnetic field less than 10 nT. Remanence measurements were made using a three-axis cryogenic magnetometer (2G Enterprises, USA) installed in a magnetically shielded space ($<$300 nT).

Results

Rock magnetic results

χ–T curves are characterized by a major drop in magnetic susceptibility at about 680 °C, the Néel temperature of hematite, indicating that hematite is the major contributor to the magnetic susceptibility (Fig. 3a, b). Stepwise IRM acquisition behaviors show that samples are unsaturated up to 1.0 T (Fig. 3c). The ratios of the isothermal remanent magnetizations obtained at a field of 0.3 T and 1.0 T ($IRM_{0.3T}/IRM_{1T}$) for NJB have a mean value of 0.56 ± 0.06 ($n = 173$; Fig. 3d). This confirms the thermomagnetic results that hematite is dominant in sediments.

Complete principal component analyses of the paleomagnetic data

Thermal magnetization is capable of isolating the characteristic remanent magnetization (ChRM) after removal of one or two soft secondary components of magnetization (Fig. 4). The principal components direction was computed by a "least-squares fitting" technique (Kirschvink, 1980). The principal component analyses (PCA) were done using the PaleoMag software (v. 3.1.0 d40) developed by Craig H. Jones and Joya Tetreault. Considering the dominance of hematite in the studied samples, we isolated the ChRM using high-temperature components. The selection criteria for reliable ChRM direction for thermally demagnetized samples include the presence of (1) a high-temperature component ($\geq$610 °C), (2) at least four demagnetization steps, and (3)
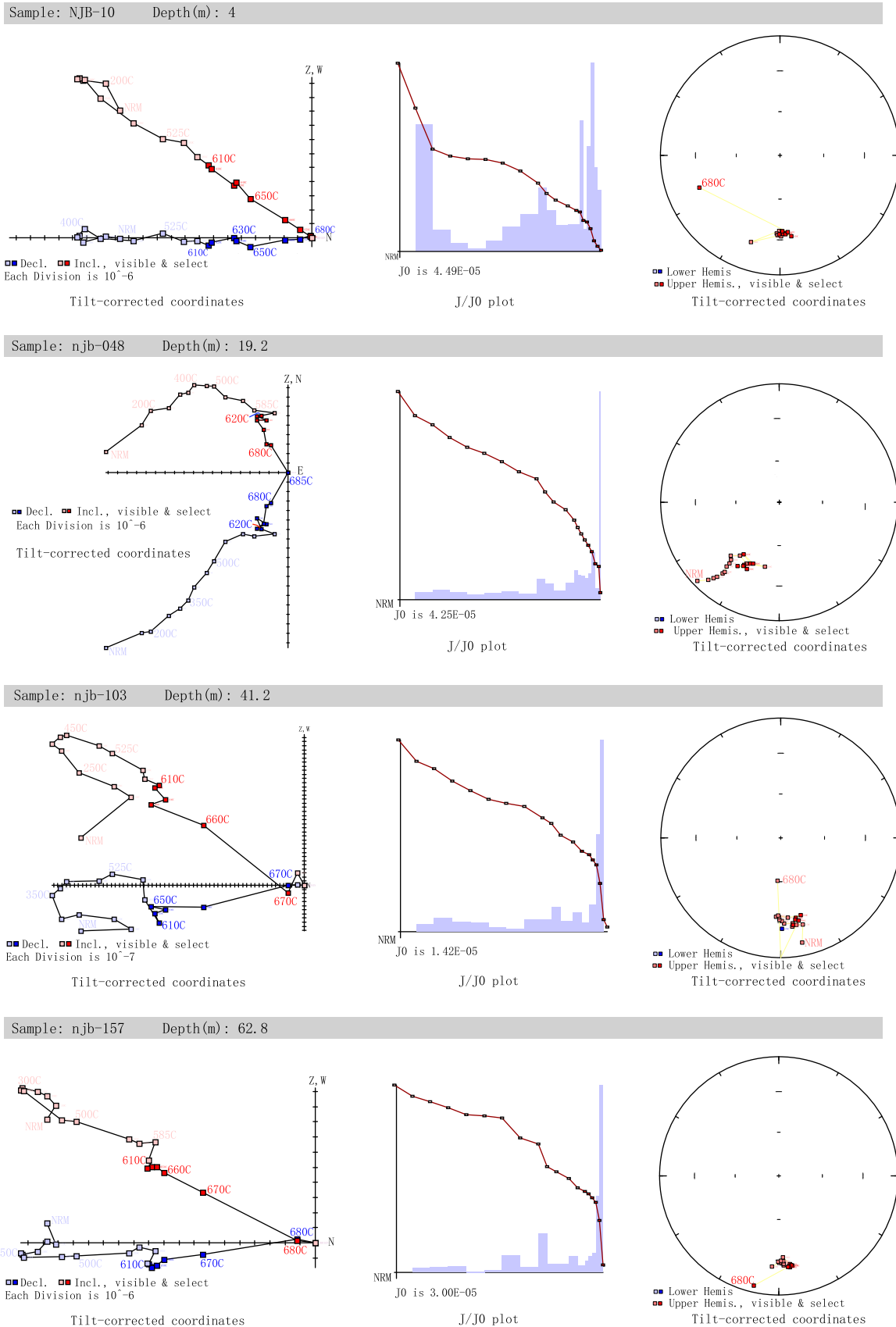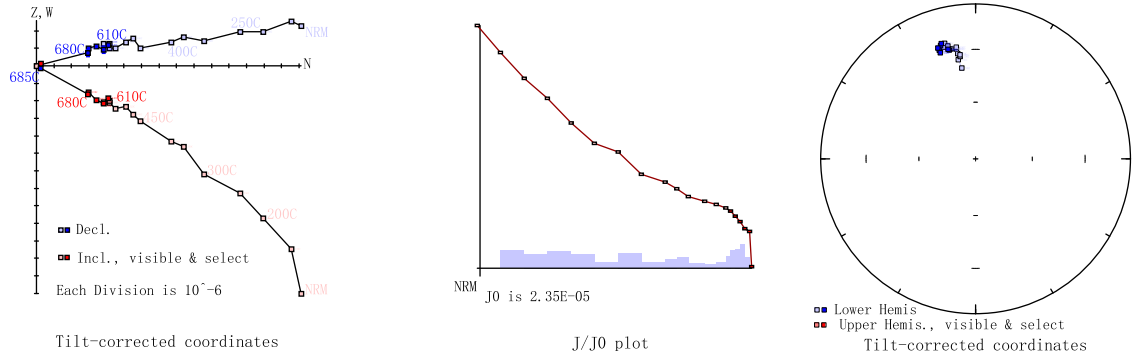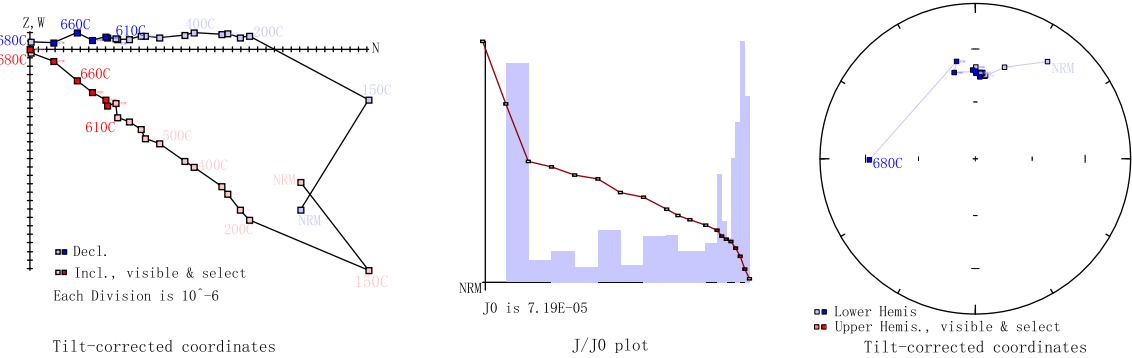
Fig. 4. Diagrams showing thermal demagnetization of the natural remanent magnetization (NRM) and corresponding orthogonal projections. The red (blue) squares represent projection of the vector on the vertical (horizontal) plane.
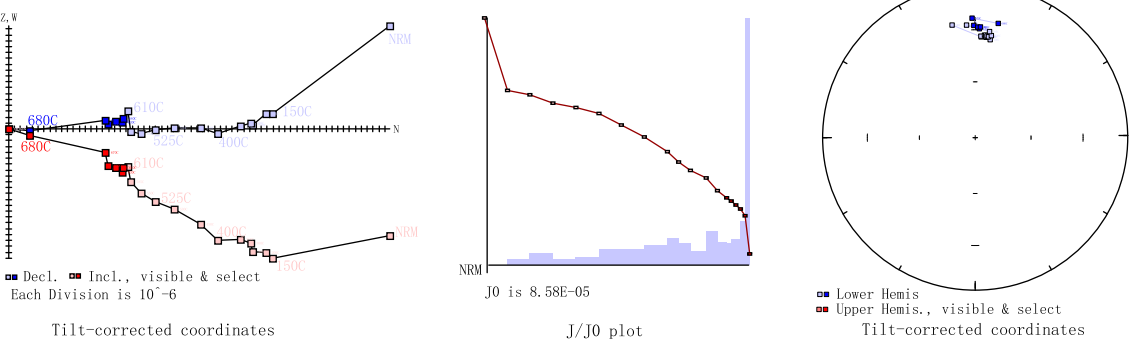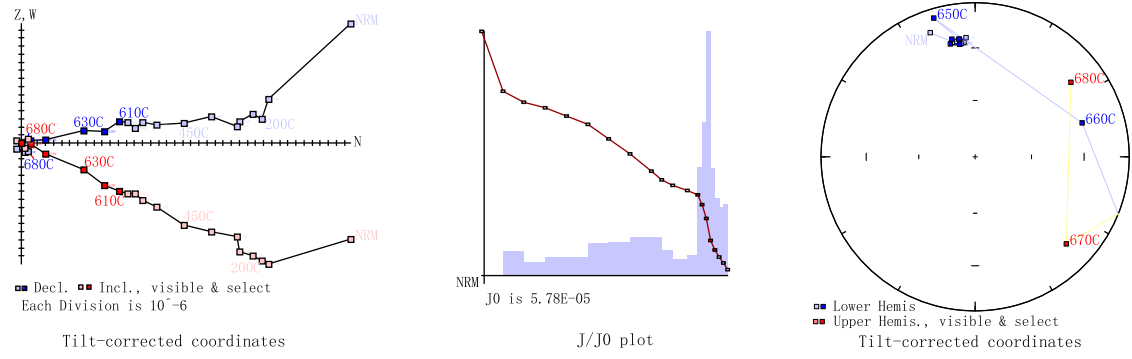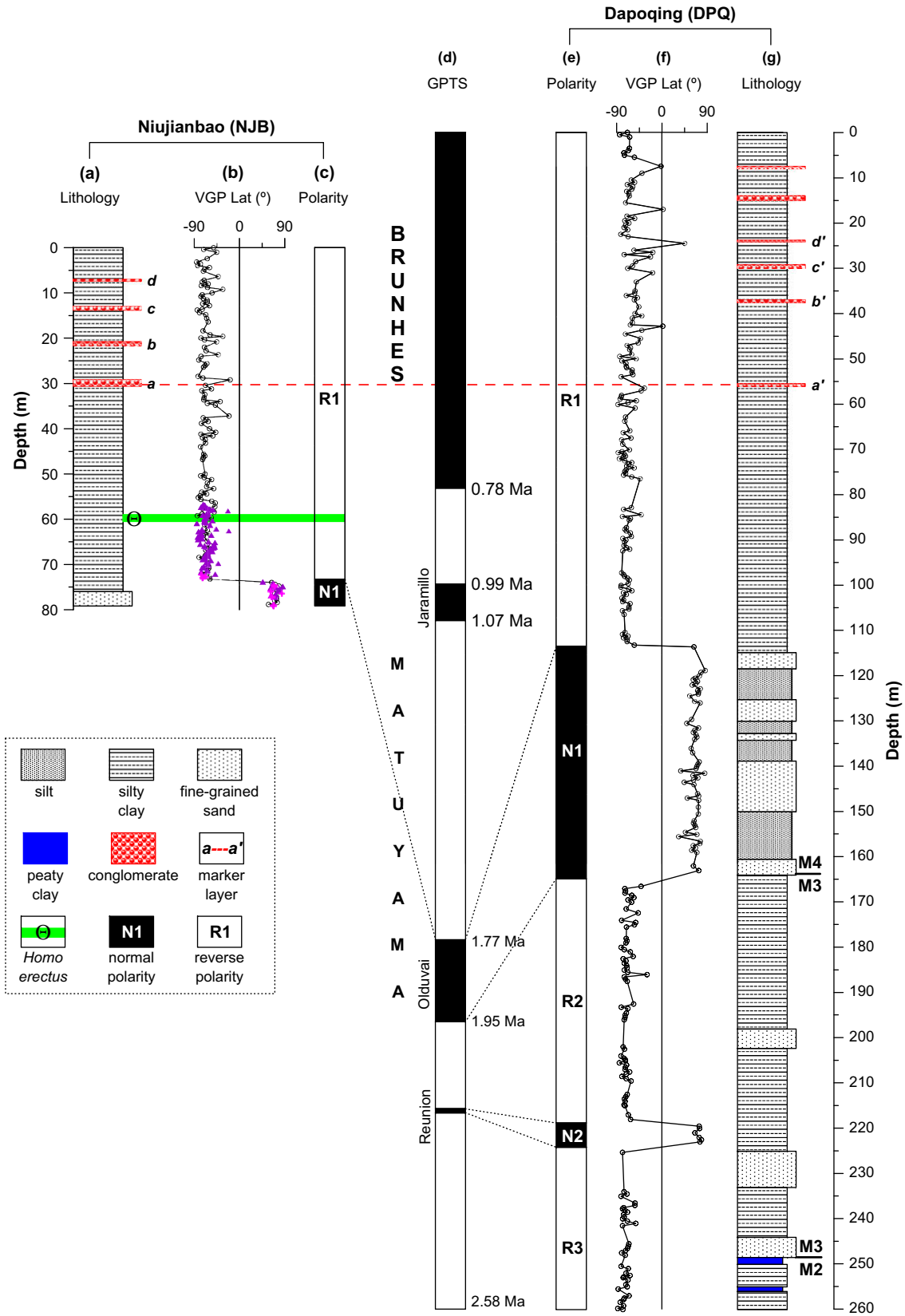
Fig. 4. (*continued*)

Fig. 5. Lithostratigraphy and magnetic polarity stratigraphy at Niujianbao (NJB; a–c) and Dapoqing (DPQ; e–g) and their correlation with the geomagnetic polarity timescale (GPTS; Berggren et al., 1995; Cande and Kent, 1995; d). The sediment layer bearing the hominin incisors (green), the marker conglomerate layer *a–a'* (red), and the lithologic member (M) boundaries are shown. VGP Lat = latitude of virtual geomagnetic pole; R = reverse polarity; N = normal polarity. Purple triangles and pink crosses in (b) represent samples from the 21-m-deep well close to the hominin site and the 8-m-deep well at the bottom of the NJB outcrop, respectively. Data of the DPQ section (e–g) are after Zhu et al. (2008).
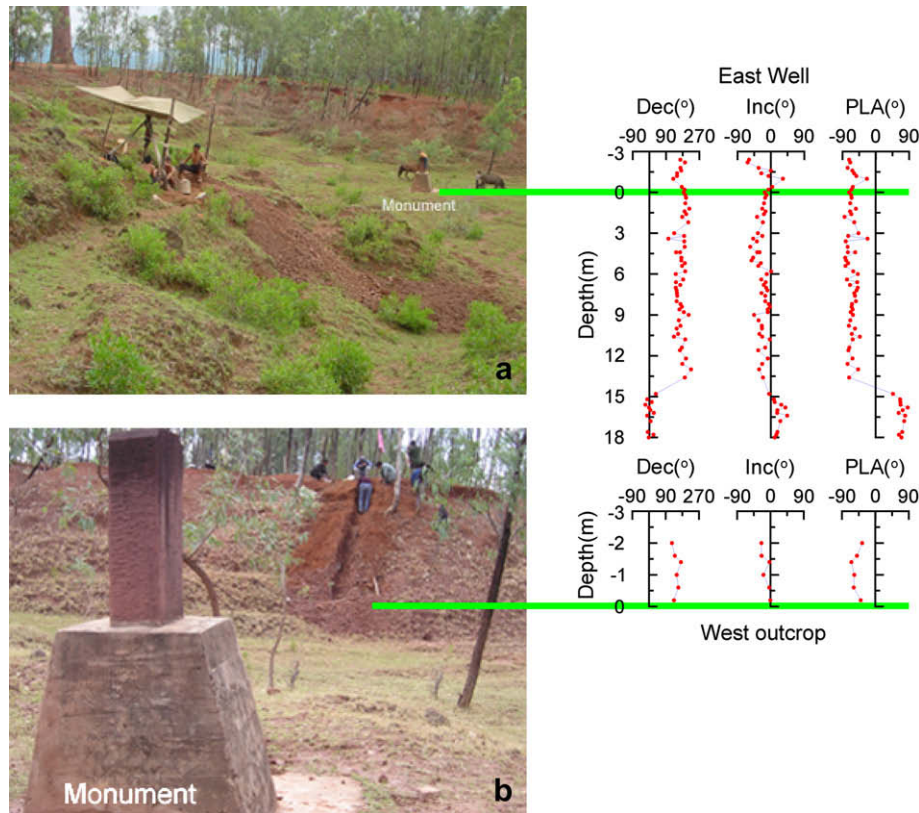
Fig. 6. *Left*: this figure shows the localities of the Yuanmou Man site (where a monument stands) and our two sampling sections adjacent to the site: the 21-m-deep well, 30 m east of the monument (a), and the outcrop section, 20 m west of the monument (b). *Right*: magnetostratigraphic profiles of the east well and west outcrop. Dec = declination; Inc = inclination; and PLA = latitude of the virtual geomagnetic pole.

a maximum angular deviation (MAD) ≤ 15°. The complete PCA results revealed 1–4 components in the studied samples and that the ChRM can be safely isolated by the high-temperature demagnetization, as suggested by the rock-magnetic investigation. In determining the ChRM data, we included the origin only if the least-squares line trended through or near the origin, but without anchoring the line through the origin for temperatures above 610 °C. Demagnetization results of representative samples were shown by orthogonal diagrams (Zijderveld, 1967) in Figure. 4. One hundred thirty-nine out of 221 samples (63%) and 68 out of 98 samples (69%) yielded reliable ChRM vectors at the NJB natural outcrop and the 21-m-deep well adjacent to the hominin site, respectively.

Magnetic polarity sequence

Following demagnetization and principal component analyses of the paleomagnetic data, the position of the virtual geomagnetic pole (VGP) for each sample layer was determined from the characteristic remanent vector direction, and the VGP latitudes were subsequently used to define the succession of magnetostratigraphic polarity (Fig. 5). The NJB section has two magnetozones: the upper one (R1, 0–73.3 m) is reverse, and the lower one (N1, 73.3–79.2 m) is normal (Fig. 5c). Specifically, the top 1 m from the west section does not yield stable ChRMs, but the remaining interval shows a reverse polarity (Fig. 6). Sediments from the east well show reverse polarity in the upper 16 m interval and normal polarity in the lower 5 m. It clearly shows that the hominin-bearing level is in a reverse polarity (Fig. 6). Therefore, both well and outcrop data show that the layer that contained the hominin incisors and stone artifacts (depth interval from 59 to 60.5 m) is confidently within

magnetozone R1, 12.8–14.3 m above the normal to reverse transition boundary (Fig. 5a–c).

Discussion

Correlations of the recognized magnetozones to geomagnetic polarity timescale

In order to better determine the age of the hominin incisors and artifacts, we compared the NJB section to a parallel section named Dapoqing (DPQ; B–B' in Fig. 1), which is located 0.5 km northwest of the NJB section and was paleomagnetically investigated in our recent study (Zhu et al., 2008). DPQ magnetozones N1 and N2 have been respectively correlated to the Olduvai and the Reunion subchrons, which were dated at 1.77–1.95 Ma and 2.14–2.15 Ma (Berggren et al., 1995; Cande and Kent, 1995), respectively; and its magnetozones R1, R2, and R3 correspond to the Matuyama reverse chron (Zhu et al., 2008). In addition, the distinctive sequence of floodplain silty clay and four conglomerate marker layers (named a–a' to d–d') can consistently be traced in the field from NJB to DPQ, thus providing a reliable stratigraphic correlation between these two sections (Fig. 5a, g). Therefore, by combining biochronological data of the NJB section (Bien, 1940; Pei, 1961; Hu, 1973; Qiu, 2000; also see Table 1), our recent magnetostratigraphic results of the DPQ section (Zhu et al., 2008; also see Fig. 5d–g), and sedimentological data of the two sections (Fig. 5a, g), the magnetozones determined for NJB can readily be correlated to the geomagnetic polarity timescale (Berggren et al., 1995; Cande and Kent, 1995). Magnetozone N1 at NJB corresponds to the late Olduvai subchron, and the hominin incisors and stone artifacts are in a reverse magnetozone, 12.8–14.3 m above the upper Olduvai-Matuyama

reversal boundary (Fig. 5a–d), which was dated at 1.77 Ma (Berggren et al., 1995; Cande and Kent, 1995).

Stratigraphic correlation and age estimation of early Homo *from Yuanmou*

The NJB section has been safely correlated with the DPQ section on sedimentological and magnetostratigraphical grounds (Fig. 5). The sediment interval between the lowest conglomerate marker layer (a–a') and the upper boundary of the Olduvai subchron mainly comprises massive fluvial silty clays interbedded with thin lenses of conglomerates. The silty clays show no development of soil formation that would indicate slowing or cessation of sedimentation. Since sampling of the DPQ and NJB sections was confined to these massive finer-grained deposits lateral to the conglomerate lenses, an overall sedimentation rate could be estimated from the deposits of a continuously aggrading floodplain.

We thus estimate the age of the a–a' layer base by extrapolating the sedimentation rates of magnetozone N1 only and magnetozones N1–R2 (that is, between the upper boundary of the Reunion subchron and the upper boundary of the Olduvai subchron) at DPQ. The average sedimentation rates of the magnetozone N1 only and magnetozones N1–R2 are 28.53 cm ka^{-1} and 28.47 cm ka^{-1}, respectively. The good agreement between the two values suggests that, on average, the sedimentation rate was relatively constant, at least so far as magnetostratigraphic age estimation is concerned.

Given that the marker layer a–a' base has a depth of 56.1 m at DPQ (Fig. 5g), the extrapolated age for this level is ~1.57 Ma. Constrained by this age for the layer a–a' base and the termination of the Olduvai subchron (1.77 Ma; Berggren et al., 1995; Cande and Kent, 1995), the average sedimentation rate for the corresponding sediment interval at NJB is 21.18 cm ka^{-1}; hence, the interpolated age estimate for the hominin incisors and stone artifact layer (12.8–14.3 m above the upper Olduvai-Matuyama reversal boundary) at NJB is 1.70 to 1.71 Ma. Given the variation in estimated sedimentation rates in the DPQ and NJB sections, we consider ~1.7 Ma as the best approximation for the age of the hominin remains.

Geochronological implications

This age estimate represents the oldest definite fossil and archaeological evidence of early hominins in China and mainland East Asia. The age is slightly younger than the earliest skeletal and archaeological evidence at Dmanisi (1.77–1.75 Ma), western Eurasia (Gabunia et al., 2000a; Vekua et al., 2002; Rightmire et al., 2006), and roughly contemporaneous with stone artifacts in the Nihewan Basin (1.66 Ma), northeast Asia (Zhu et al., 2004), and with the oldest known hominin fossils in Java (1.5–1.8 Ma), southeast Asia (Swisher et al., 1994; Larick et al., 2001; Antón and Swisher, 2004). Since the oldest date relevant to fossil hominins in southeast Asia, ~1.81 Ma for the Mojokerto fossil (Swisher et al., 1994), is located about 20 m beneath the likely original stratum of the fossil (Huffman et al., 2006), the estimate of 1.7 Ma obtained here for the Yuanmou artifacts and fossils may represent a roughly equivalent age or possibly slightly older evidence of hominins in East Asia.

Paleoenvironmental context

Paleoenvironmental evidence directly associated with the Yuanmou hominins comes from fossil fauna and microbotanical remains. The associated fauna (Table 1) includes 35 mammal taxa and various mollusks, fish, and turtle. Twenty-one of the 35 taxa (for example, *Equus yunnanensis*) are taxonomically affiliated with typical grazing species indicative of an open grassland environment. The occurrence of *Rhizomys* sp., *Sus* sp., *Nestoritherium*

(*Hesperotherium*) sp., and *Viverricula malaccensis fossilis* probably indicates bushland, while the presence of *Megantereon nihowanensis*, *Stegodon elephantoides*, and *Stegodon* sp. suggests forest habitat. The occurrence of numerous mollusks indicates a low-energy lakeshore or marsh setting, and the presence of *Cyriuus caspio* and *Testudo* sp. is characteristic of a perennial open aquatic environment. Fossil pollen recovered in the sedimentary layer bearing the Yuanmou incisors and artifacts is dominated by *Pinus* (33.3%), *Alnus* (13%), and herbaceous vegetation (40%; Pu and Qian, 1977; Qian and Zhou, 1991), indicating locally-extensive herbaceous cover with patches of forest surrounding the paleolake or paleoswamp. In sum, the faunal assemblage and pollen from the hominin site indicate that Yuanmou *Homo* lived in an area with a diversity of habitats that included open grassland, bushland, forest, marsh, and fresh water. A very similar environmental setting is reconstructed for the 1.77-Ma hominins at Dmanisi, characterized as a lake or pond surrounded by diverse vegetation and faunal resources (Gabunia et al., 2000b).

Paleoanthropological significance

As noted earlier, the Yuanmou incisors show strong morphological and metrical similarities to upper central incisors of early African *H. erectus* sensu lato and *H. habilis*. In addition, the Yuanmou stone artifacts exhibit simple yet precise conchoidal fracture typical of African Oldowan technology. The Yuanmou finds thus suggest the African affinities of both the dental morphology and stone flaking behavior of the earliest recorded East Asian hominins.

The convergence of age estimates at 1.70–1.66 Ma for the oldest currently known paleoanthropological evidence from south China (Yuanmou), north China (Nihewan), and Southeast Asia (Sangiran; possibly Mojokerto) has further implications with varying degrees of reliability. First, the evidence of *Homo* at Yuanmou roughly 70 kyr after the age of the Dmanisi hominins might imply that *Homo*, once it dispersed beyond Africa, spread rapidly across Asia during the earliest Pleistocene. Second, the location of the earliest known hominins of mainland East Asia in the subtropical Yuanmou Basin is consistent with a southern route of movement into East Asia from Africa. These two possibilities remain highly uncertain, however, due to the very small sample of well-dated sites with definite evidence of *Homo* and/or stone artifacts in Eurasia near the Pliocene-Pleistocene boundary.

The similarity of age constraints (1.70–1.66 Ma) currently defined for different areas of eastern Asia may yield, however, a more robust hypothesis concerning this novel extension of the geographic range of *Homo*. Early *Homo* at Yuanmou lived near the time of a wide expansion of East Asian hominins over an area that extended from at least 40°N (Nihewan Basin) to 7°S (Java) latitude, across a habitat range from temperate grassland to tropical woodland and possibly forest (Zhu et al., 2003, 2004; Antón and Swisher, 2004). The oldest recorded hominin dispersal to East Asia apparently culminated in the ability to adapt to a wide variety of environments and, eventually, the lengthy persistence of *H. erectus* in East Asia prior to *H. sapiens*.

Conclusions

The NJB sedimentary sequence in the Yuanmou Basin, southwest China, which contains the Yuanmou hominin fossils and stone artifacts, recorded the Olduvai subchron and a reverse magnetozone above the upper Olduvai-Matuyama reversal boundary. The hominin-bearing layer resides in the reverse polarity magnetozone just above the upper boundary of the Olduvai subchron, yielding an estimated age of 1.7 Ma. The finding represents the age of the earliest documented arrival of the genus *Homo* in mainland East Asia. The Yuanmou hominins encountered a varied habitat of open

vegetation with patches of bushland and forest on an alluvial fan close to a lake or swamp. The age, paleoenvironmental evidence, and similarity of the Yuanmou incisors and artifacts to East African finds are consistent with the expansion of African-derived *Homo* into environmentally diverse regions of eastern Asia during the earliest Pleistocene.

Acknowledgements

References

Antón, S.C., Swisher III, C.C., 2004. Early dispersals of *Homo* from Africa. Annu. Rev. Anthropol. 33, 271–296.

Berggren, W.A., Kent, D.V., Swisher III, C.C., Aubry, M.-P., 1995. A revised Cenozoic geochronology and chronostratigraphy in time scales and global stratigraphic correlations: a unified temporal framework for an historical geology. In: Berggren, W.A., Kent, D.V., Aubry, M.-P., Hardenbol, J. (Eds.), Geochronology, Timescales, and Stratigraphic Correlation, Spec. Publ. No. 54. Society of Economic Paleontologists and Mineralogists, Tulsa, OK, pp. 129–212.

Bien, M.N., 1940. Preliminary observation on the Cenozoic geology of Yunnan. Bull. Geol. Soc. China 20, 179–194.

Cande, S.C., Kent, D.V., 1995. Revised calibration of the geomagnetic polarity timescale for the Late Cretaceous and Cenozoic. J. Geophys. Res. 100(B4), 6093–6096.

Deng, C.L., Zhu, R.X., Zhang, R., Ao, H., Pan, Y.X., 2008. Timing of the Nihewan formation and faunas. Quatern. Res. 69, 77–90.

Dennell, R., 2003. Dispersal and colonisation, long and short chronologies: how continuous is the Early Pleistocene record for hominids outside East Africa? J. Hum. Evol. 45, 421–440.

Dennell, R., Roebroeks, W., 2005. An Asian perspective on early human dispersal from Africa. Nature 438, 1099–1104.

Gabunia, L., Vekua, A., Lordkipanidze, D., Swisher III, C.C., Ferring, R., Justus, A., Nioradze, M., Tvalchrelidze, M., Antón, S.C., Bosinski, G., Jöris, O., -de Lumley, Marie A., Majsuradze, G., Mouskhelishvili, A., 2000a. Earliest Pleistocene hominid cranial remains from Dmanisi, Republic of Georgia: taxonomy, geological setting, and age. Science 288, 1019–1025.

Gabunia, L., Vekua, A., Lordkipanidze, D., 2000b. The environmental contexts of early human occupation of Georgia (Transcaucasia). J. Hum. Evol. 38, 785–802.

Hu, C.Z., 1973. Ape-man teeth from Yuanmou, Yunnan. Acta Geol. Sin. 1, 65–72.

Huffman, O.F., Zaim, Y., Kappelman, J., Ruez Jr., D.R., Rizal, Y., Aziz, F., Hertler, C., de Vos, J., 2006. Relocation of the 1936 Mojokerto skull discovery site near Perning, East Java. J. Hum. Evol. 50, 431–451.

Hyodo, M., Nakaya, H., Urabe, A., Saegusa, H., Xue, S., Yin, J., Ji, X., 2002. Paleomagnetic dates of hominid remains from Yuanmou, China, and other Asian sites. J. Hum. Evol. 43, 27–41.

Kirschvink, J.L., 1980. The least-squares line and plane and analysis of palaeomagnetic data. Geophys. J.R. Astron. Soc. 62, 699–718.

Larick, R., Ciochon, R.L., Zaim, Y., Suminto, S., Rizal, Y., Aziz, F., Reagan, M., Heizler, M., 2001. Early Pleistocene $^{40}Ar/^{39}Ar$ ages for Bapang formation hominins, Central Java, Indonesia. Proc. Natl. Acad. Sci. 98, 4866–4871.

Li, P., Qian, F., Ma, X., Pu, Q., Xing, L., Ju, S., 1976. Preliminary study on the age of the Yuanmou Man by paleomagnetic technique. Science in China 6, 579–591 (in Chinese).

Lin, Y.P., Pan, Y.R., Lu, Q.W., 1978. Early Pleistocene mammalian fauna in the Yuanmou basin, Yunnan Province. In: Institute of Vertebrate Paleontology and Paleoanthropology Contributions to Paleoanthropology. Science Press, Beijing, pp. 101–125.

Liu, W., Zheng, L., Jiang, C., 2000. Statistical analyses of metric data of hominoid teeth found in Yuanmou of China. Chin. Sci. Bull. 45, 936–942.

Lordkipanidze, D., Jashashivili, T., Vekua, A., Ponce de León, M.S., Zollikofer, C.P.E., Rightmire, G.P., Pontzer, H., Ferring, R., Oms, O., Tappen, M., Bukhsianidze, M., Agusti, J., Kahlke, R., Kiladze, G., Martinez-Navarro, B., Mouskhelishvili, A., Nioradze, M., Rook, L., 2007. Postcranial evidence from early *Homo* from Dmanisi, Georgia. Nature 449, 305–310.

Pei, W.C., 1961. Fossil mammals of early Pleistocene age from Yuanmo (Ma-kai) of Yunnan. Vertebrata Palasiatica 3(1), 16–31.

Pilbrow, V., 2006. Lingual incisor traits in modern hominoids and an assessment of their utility for fossil hominoid taxonomy. Am. J. Phys. Anthropol. 129, 323–338.

Pu, Q.Y., Qian, F., 1977. Study on the fossil human strata—the Yuanmo Formation. Acta. Geol. Sin. 1, 89–100.

Qian, F., Pu, Q.Y., Wang, D.S., 1984. The discovery of the teeth of Yuanmou Man. In: Zhou, G.X., Zhang, X.Y. (Eds.), Yuanmou Man. Yunnan People's Press, Kunming, pp. 3–7.

Qian, F., Zhou, G.X., 1991. Quaternary Geology and Paleoanthropology of Yuanmou, Yunnan, China. Science Press, Beijing.

Qiu, Z.X., 2000. Nihewan fauna and Q/N boundary in China. Quatern. Sci. 20, 142–154 (in Chinese with English abstract).

Rightmire, G.P., Lordkipanidze, D., Vekua, A., 2006. Anatomical descriptions, comparative studies and evolutionary significance of the hominin skulls from Dmanisi, Republic of Georgia. J. Hum. Evol. 50, 115–141.

Singer, B.S., Relle, M.K., Hoffman, K.A., Battle, A., Laj, C., Guillou, H., Carracedo, J.C., 2002. Ar/Ar ages from transitionally magnetized lavas on La Palma, Canary Islands, and the geomagnetic instability timescale. J. Geophys. Res. 107, 2307, doi:10.1029/2001JB001613.

Swisher III, C.C., Curtis, G.H., Jacob, T., Getty, A.G., Suprijo, A., Widiasmoro, 1994. Age of the earliest known hominids in Java, Indonesia. Science 263, 1118–1121.

Tocheri, M.W., Orr, C.M., Larson, S.G., Sutikna, T., Jatmiko, Saptomo, E.W., Due, R.A., Djubiantono, T., Morwood, M.J., Jungers, W.L., 2007. The primitive wrist of *Homo floresiensis* and its implications for hominin evolution. Science 317, 1743–1745.

Vekua, A., Lordkipanidze, D., Rightmire, G.P., Agusti, J., Ferring, R., Maisuradze, G., Mouskhelishvili, A., Nioradze, M., Ponce de Leon, M., Tappen, M., Tvalchrelidze, M., Zollikofer, C., 2002. A new skull of early *Homo* from Dmanisi, Georgia. Science 297, 85–89.

Walker, A., Leakey, R., 1993. The Nariokotome *Homo erectus* Skeleton. Harvard University Press, Cambridge, M.A.

Wen, B.H., 1978. Paleolithic stone tools found in the Yuanmou Basin, Yunnan Province. In: Institute of Vertebrate Paleontology and Paleoanthropology Contributions to Paleoanthropology. Science Press, Beijing, pp. 126–135.

Wood, B., 1991. Koobi Fora Research Project Volume 4, Hominid Cranial Remains. Clarendon, Oxford.

Wood, B.A., Xu, Q., 1991. Variation in the Lufeng dental remains. J. Hum. Evol. 20, 291–311.

Worm, H.-U., 1997. A link between geomagnetic reversals and events and glaciations. Earth Planet. Sci. Lett. 147, 55–67.

Wu, X., Poirier, F.E., 1995. Human Evolution in China: A Metric Description of the Fossils and a Review of the Sites. Oxford University Press, New York.

Yuan, Z.X., Lin, Y.P., Zhou, G.X., Zhang, X.Y., Wen, B.H., Jiang, C., Zhao, P., Zhang, G.Y., Wei, H.K., 1984. Field report of an excavation at Yuanmou Man's site. In: Zhou, G.X., Zhang, X.Y. (Eds.), Yuanmou Man. Yunnan People's Press, Kunming, China, pp. 12–22.

Zhu, R.X., An, Z.S., Potts, R., Hoffman, K.A., 2003. Magnetostratigraphic dating of early humans in China. Earth-Sci. Rev. 61, 341–359.

Zhu, R.X., Potts, R., Pan, Y.X., Lü, L.Q., Yao, H.T., Deng, C.L., Qin, H.F., 2008. Paleomagnetism of the Yuanmou Basin near the southeastern margin of the Tibetan Plateau and its constraints on late Neogene sedimentation and tectonic rotation. Earth Planet. Sci. Lett. 272, 97–104.

Zhu, R.X., Potts, R., Xie, F., Hoffman, K.A., Deng, C.L., Shi, C.D., Pan, Y.X., Wang, H.Q., Shi, R.P., Wang, Y.C., Shi, G.H., Wu, N.Q., 2004. New evidence on the earliest human presence at high northern latitudes in northeast Asia. Nature 431, 559–562.

Zijderveld, J.D.A., 1967. A.C. demagnetization of rocks: analysis of results. In: Collinson, D.W., Creer, K.M., Runcorn, S.K. (Eds.), Methods in Paleomagnetism. Elsevier, New York, pp. 254–286.